Desalination and Water Treatment
www.deswater.com

doi: 10.1080/19443994.2014.989272

57 (2016) 3835–3845
February

Taylor & Francis
Taylor & Francis Group

DCMD modelling and experimental study using PTFE membrane

Khaled Nakoa[a,b,c,*], Abhijit Date[a,c], Aliakbar Akbarzadeh[a,c]

[a]*Aerospace, Manufacturing and Mechanical Engineering, RMIT University, Melbourne, Victoria, Australia, Tel. +61 3 9925 6224; email: s3302136@student.rmit.edu.au (K. Nakoa), Tel. +61 3 9925 0612; email: abhijit.date@rmit.edu.au (A. Date), Tel. +61 3 9925 6079; email: aliakbar.akbarzadeh@rmit.edu.au (A. Akbarzadeh)*
[b]*Jado Engineering Faculty, Al Jabal Al Gharbi University, Jado, Al Jabal Al Gharbi, Libya*
[c]*RMIT Energy CARE Group*

Received 31 March 2014; Accepted 10 November 2014

ABSTRACT

This research work aims to investigate the performance of direct contact membrane distillation (MD) unit under different conditions. A mathematical model was developed to evaluate the experimental values of the membrane water mass flux, heat transfer coefficients, the membrane/liquid interface temperatures, the temperature polarisation coefficient and the evaporation efficiency. This model was solved numerically using MATLAB® software, and its results were used to predict the actual performance of the membrane unit. The MD coefficient was evaluated from the computer model data and was subsequently used to estimate water fluxes. Experimental tests were performed using 0.0572 m^2 of PTFE membrane manufactured by membrane solution (85% porosity, 45 μm thickness, 0.22 μm nominal pore size). Feed solutions were aqueous NaCl solutions with 1,000–200,000 mg/L (0.1–20%) in concentration and its temperatures were 40–80˚C, and feed flow rate was 2 L/min. The temperature and flow rate of permeate water was fixed at 20˚C and 3 L/min, respectively. The experimental observation showed that the vapour mass flux through the membrane pores increased with feed temperature, but decreased with feed concentration. It was found that the predicted mass fluxes agreed reasonably with the experimental data, except at a high feed concentration. The temperature polarisation coefficients increased with concentration and decreased with increasing temperature. The membrane heat transfer rates and the permeate flux have been discussed in this paper.

Keywords: Membrane distillation; Water desalination; Membrane distillation coefficient; Permeate mass flux

1. Introduction

Since 1950, global demand for freshwater has approximately doubled every 15 years. About 450 million people in 29 countries face severe water shortages; about more than 20% water now available will be needed to feed the additional three billion people by 2025 [1]. This growth has reached a point where today existing freshwater resources are under great stress, and it has become both more difficult and more expensive to develop new freshwater resources. One, especially, relevant issue is that a large proportion of the world's population (approximately 70%) dwells in coastal zones [2]. Furthermore, the World Health

*Corresponding author.

Organization reported that 20% of the world population has inadequate drinkable water. Even though the two-third of the planet is covered with water, 99.3% of this water either has high salinity or not accessible (Ice caps) [3]. The current mean population density at coastlines is almost 100 hab/km^2, and it is over 2.5 times the global average and embraces 45% of the global population [4]. Many of these coastal regions rely on underground aquifers for a substantial portion of their freshwater supply. In particular, if the aquifer is overdrawn, it can be contaminated by an influx of seawater or salts and, therefore, requires a treatment or purification. So, the combined effects of increasing freshwater demand, population growth and seawater intrusion into coastal aquifers are stimulating the demand for desalination.

Desalination is a process of removing salts and other minerals from a saline water solution producing fresh water, which is suitable for human consumption, agriculture and industrial use. The desalination system usually consists of three main parts; water source, desalination unit and energy source, which are playing a key role in evaluating the desalination plant performance. The desalination systems can be classified into three categories; thermal process that uses phase change such as multi-effect desalination and multi-stage flash; membrane process that uses a certain membrane without liquid phase change such as, reverse osmosis (RO) and electrodialysis, the third one is a hybrid system that involves two processes, phase change and membrane technology such as thermal membrane distillation (MD).

The MD membrane is defined as a thin microporous barrier between two solutions which allows only the volatile molecules to pass through its pores. Furthermore, hydrophobic microporous membrane is the preferable membrane type that is used with MD. MD is a thermally driven process that has hot and cold streams at both sides of the membrane, and it can produce high pure water from saline or waste water. The vapour–liquid interface forms at the pore entrance on the hot feed side then, the volatile components such as vapour diffuse through the pore and condense at the cold permeate side. The driving force of the vapour is the hydrostatic pressure difference resulted from the temperature difference between hot and cold membrane surfaces.

The invention of membrane was in 1963 by Bodell. In 1967, first paper about MD was published by Findley [5]. The death phase of MD research occurred from 1970 to 1980 as indicated by no reported study can be found [6]. In 1980s, a new membrane with better characteristics has become available [7]. A number of researchers and intensive works performed on MD have been increased noticeably from late 1990s to 2005, resulted in a major advancement and present different MD configuration [7]. Furthermore, the capability to utilise the low-grade heat source such as waste heat, geothermal or solar energy with MD, makes it more promising future technology.
Some MD benefits are:

(1) It can produce freshwater at low temperature that is provided by low-grade heat source such as solar energy, waste heat, and geothermal.
(2) High salt rejection can be achieved.
(3) It can work near to the saturated concentration.
(4) It works at low hydrostatic pressure.
(5) Pre-treatment is cost effective compared to RO process.
(6) Less sensitive to feed characteristics (PH, TDS, etc.).

Even though MD has some advantages over other desalination technology, using MD commercially still need to be more investigated, and it should be implemented in the industrial sector with large-scale and long-term application. MD can be commercialised if these requirements are satisfied:

(1) High liquid entry pressure (LEP).
(2) High permeability.
(3) Low thermal conductivity.

Mainly, there are four commercial membranes that can be used with MD available in the market. They are polypropylene, polyvinylidene fluoride, Polytetrafluoroethylene (PTFE) and polyethylene which are available in tubular, capillary and flat sheet forms.

MD process had become more interested when improved membranes and modules with better characteristics became available in the market. Furthermore, the combination with MD capability to utilise low-grade temperature of alternative energy sources, such as solar and geothermal energy, have stimulated the advances in MD technique [8]. The importance of MD as a useful desalination technique can be detected from the increasing number of published papers available in the literature recently. However, from a commercial point of view, MD is not implemented yet in the industry. The relatively low permeate flux and high and uncertain energy, and economic costs are the main barriers to commercial implementation of MD and preventing it from being a viable desalination technology.

Researchers studied many MD modules and factors affecting MD distilled water production associated with some applications of enhancement techniques [9,10]. For instance, MD is suited for pro-

duction of distilled water and concentration of aqueous solutions. MD has been applied for water desalination, a chemical solution treatment, environmental waste clean-up, water reuse and food processing [11]. Also, used among other applications such as milk and juice concentration, and biomedical applications. Moreover, it has been used for separation of azeotropic aqueous mixtures such as alcohol–water mixtures, concentration of radioactive solutions and application for nuclear desalination [12]. In many applications, it can be used for treatment of humic acid solutions, pharmaceutical waste water and in areas where high-temperature applications lead to degradation of process fluids [13]. It must be known that desalination is the most known direct contact membrane distillation (DCMD) application as nearly 99% rejection of non-volatile molecules solutions is easily achieved.

2. Membrane configurations

The membrane configuration is defined as the method of recovering the vapour after it has immigrated through membrane pores. The oldest membrane method is DCMD where liquid phases are in direct contact with both surfaces of the membrane as shown in Fig. 1. The alternative methods are air gap membrane distillation (AGMD), vacuum membrane distillation and sweeping gas membrane distillation [5].

3. Membrane characteristics

Different types of membranes have been developed and manufactured for many years. For more understanding of membrane behaviour, researchers investigate characteristics of membranes such as porosity or pore size, thickness and material. Also, they study the effects of the fluid properties that are used with MD and the flow conditions through the system.

The membrane has different characteristics affecting its performance and mass flux such as porosity, pore size. The porosity is the ratio between the pore size and the solid size of the membrane. It varies between 30 and 85%, and it has a significant effect on membrane mass flux or transmembrane parameter [7]. Furthermore, the pore size which is ranging between 100 nm and 1 μm, has the same effect on membrane mass flux. If the membrane pore size increases, the transmembrane increases and vice versa. Another character is the pore distribution in the membrane surface, but its effect on MD flux has not been sufficiently investigated. Finally, the effect of membrane material and thickness are still under investigation. Membranes may produce more freshwater by choosing appropriate material with low surface energy, pore size and high hydrophobicity [5]. In general, membrane area does not have a significant effect on the flux rate, but it lowers the specific energy consumption substantially [14].

Another aspect is the heat transfer and flow conditions, adjacent the membrane surface where the hot and cold fluid comes in contact with it. MD mass flux increases with feed mass flow velocity and reaches

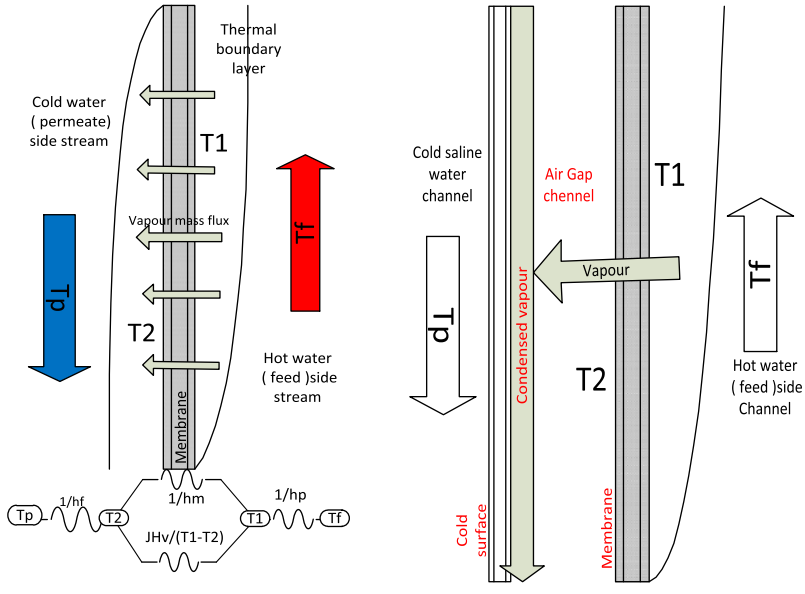

Fig. 1. Heat boundary layers and thermal resistance at the membrane sides for DCMD and AGMD.

asymptotic level at higher rates. Also, the membrane hydrostatic pressure must be lower than the LEP of hot side solution to avoid pore wetting that can be achieved by working under turbulent flow. The permeate flux increases with feed temperature, the temperature difference and permeate side flow velocity [7]. They affect the heat transfer coefficient which is consequently affecting the mass flux.

4. Theoretical approach

The driving force in MD is the transmembrane vapour pressure, which can be applied in the DCMD by a temperature difference between the feed and permeate side of the membrane module. The different vapour pressures at both membrane sides force the vapour molecules to travel through the membrane pores. Therefore, from Fig. 1 (T_1) is the evaporation feed/membrane interface temperature and T_2 is the condensation permeate/membrane interface temperature.

4.1. Flow mechanisms

There are three basic mechanisms of mass flow inside the membrane wall, which are Knudsen diffusion, Poiseuille flow and molecular diffusion. In Knudsen diffusion, the pore size is too small, and the collision between molecules can be neglected. Furthermore, the collision between sphere molecules and the internal walls of the membrane is the dominant mass transport form. Molecular diffusion occurs if the pore size is big comparing to the mean free path of molecules and they move corresponding to each other. The flow is considered Poiseuille (viscous flow), if the molecules act as a continuous fluid inside the membrane pores. In general, different mechanisms occur simultaneously (Knudsen, Poiseuille and molecular diffusion) inside the membrane if the pore size is less than 0.5 μm [15].

4.1.1. Knudsen number

It is a governing quantity of the flow mechanism inside the membrane pores which is the ratio between the mean free path of the transported molecules and the pore size of the membrane. For an instant, the mean free path for water vapour at 50°C under atmospheric pressure is approximately 0.14 μm [5]. The Knudsen number Kn defined in the following equation and is used to determine the dominating mechanism of mass transfer inside the pore:

$$\mathrm{Kn} = \frac{S}{d} \tag{1}$$

S is the mean free path of the transferred gas molecule and d is the mean pore diameter of the membrane.

S is calculated from:

$$S = \frac{k_B T}{\sqrt{2}\pi P d_e^2} \tag{2}$$

k_B, T and P are Boltzmann constant (1.380622×10^{-23} J/K), absolute temperature and average pressure inside the membrane pores, respectively. d_e is the collision diameter of the water vapour and air that are 2.64×10^{-10} m and 3.66×10^{-10} m, respectively [15].

The pore sizes of the most membranes are in the range of 0.2–1.0 μm. The mean free path of water vapour is 0.11 μm at feed temperature of 60°C. Therefore, Kn is the range of 0.11–0.55.

The different flow mechanisms inside the membrane pores can be identified by Knudsen number (Kn):

$\mathrm{Kn} < 0.01$	molecular diffusion.
$0.01 < \mathrm{Kn} < 1$	Knudsen-molecular diffusion transition mechanism
$\mathrm{Kn} > 1$	Knudsen mechanism

4.1.2. Mass flux (J)

As shown in Fig. 1, vapour in transferring from feed side of the membrane to the permeate side by pressure difference force, which results from the temperature difference between the two sides. The mass transfer may be written as a linear function of the vapour pressure difference across the membrane, given by

$$J = C_m(P_1 - P_2)\ \mathrm{kg/m^2/s} \tag{3}$$

where J is the mass flux, C_m is the MD coefficient, and P_1, P_2 are the partial pressures of water vapour evaluated at the membrane surface temperatures T_1, T_2.

C_m for Knudsen flow mechanisms:

$$C_m^k = \frac{2\varepsilon r}{3\tau\delta}\left(\frac{8M}{\pi RT}\right)^{1/2} \tag{4}$$

C_m for molecular diffusion

$$C_m^D = \frac{\varepsilon}{\tau\delta}\frac{PD}{P_a}\frac{M}{RT} \tag{5}$$

C_m for Knudsen-molecular diffusion transition mechanism:

$$C_m^C = \left[\frac{3}{2}\frac{\tau\delta}{\varepsilon d}\left(\frac{\pi RT}{8M}\right)^{1/2} + \frac{\tau\delta}{\varepsilon}\frac{P_a}{PD}\frac{RT}{M}\right]^{-1} \quad (6)$$

D is the diffusion coefficient of the vapour in the air. P is the pressure at $\bar{T}$ and can be found using Antoine equation:

$$P = \exp\left(23.238 - \frac{3,841}{\bar{T} - 45}\right) \quad (7)$$

where $\bar{T}$ is the average temperature between feed and permeate side, which is assumed to be inside the membrane pores.

4.2. Heat flux (q)

The heat transfer models of MD can be summarised as follows:

(1) Convective heat transfer from the feed side to the membrane surface:

$$q_f = h_f(T_f - T_1) \quad (8)$$

where q_f is the feed heat flux (W/m^2) and h_f is the heat transfer coefficient (W/m^2 K).

(2) Heat flux through the membrane that includes conduction heat flux through the solid material of the membrane $k_m \frac{dt}{dx}$ and the latent heat transfer as a conviction by water vapour through the pores JH_v:

$$q_m = JH_v + k_m \frac{dT}{dx} \quad (9)$$

H_v is the vaporization enthalpy of water evaluated at the mean temperature $\frac{T_1+T_2}{2}$, and the second term is the conduction heat loss through the membrane material.

Finally, heat is transferred through the permeate boundary layer to the permeate water by convection.

$$q_p = h_p(T_2 - T_p) \quad (10)$$

At steady state:

$$q_f = q_m = q_p \quad (11)$$

The overall heat transfer coefficient can be determined by:

$$U = \left[\frac{1}{h_f} + \frac{1}{\frac{k_m}{\delta_m} + \frac{JH_v}{T_1 - T_2}} + \frac{1}{h_p}\right]^{-1} \quad (12)$$

The rate of total heat transferred through the membrane is:

$$q_t = U(T_f - T_p) \quad (13)$$

The feed flow energy balance is:

$$q_f = \dot{m}_f c_p (T_{f,in} - T_{f,out}) \quad (14)$$

The thermal efficiency of the membrane is:

$$E_t(\%) = \frac{JH_v A}{Q_t} \times 100 \quad (15)$$

The thermal efficiency is the ratio between the water heat energy consumption to generate vapour and the total heat energy supplied to the system. Whereas, heat conduction through membrane solid, is considered heat loss and it should be minimised.

The efficiency should include both thermal and electrical energy (pumps), thus gained output ratio (GOR) can define it as:

$$\mathrm{GOR} = \frac{JH_v A}{E_T + E_E} \quad (16)$$

To determine heat transfer coefficients of the boundary layers at both membrane sides, the average bulk temperature of feed side $\frac{T_f+T_1}{2}$, and at permeate side $\frac{T_2+T_p}{2}$ of the membrane should be used. Graetz–Leveque correlation is recommended [16]:

$$\mathrm{Nu} = 1.86\left(\mathrm{RePr}\frac{d_h}{L}\right)^{0.33} \quad d_h = \frac{4A_c}{P_e} \quad (17)$$

This correlation can be used for laminar flow (Re < 2,100).

In contrast, next correlation can be applied for turbulent flow ($2,500 < \mathrm{Re} < 1.25 \times 10^5$ and $0.6 < P_r < 100$).

$$\mathrm{Nu} = 0.023\ \mathrm{Re}^{0.8}\ \mathrm{Pr}^{n} \tag{18}$$

where n is equal to 0.4 for heating and 0.3 for cooling [17].

The dimensionless groups, Nusselt number (Nu), Reynolds number (Re) and Prandtl number (Pr) can be calculated using the available physical data of feed and permeate fluid.

At both sides of the membrane where the vapour–liquid interface takes place, there is a thermal boundary layer which has a temperature difference from the bulk stream. The difference is described as temperature polarisation coefficient (TPC) or (λ).

$$\lambda = \frac{T_1 - T_2}{T_f - T_p} \tag{19}$$

The iterative method by a computer program is applied to predict T_1 and T_2 as shown in Fig. 2, and a sample of model theoretical results are shown in Table 1.

$$H_v \text{ is evaluated at } TT = \frac{T_1 + T_2}{2} \tag{20}$$

Finally,

$$T_1 = \frac{h_m\left(T_p + \left(h_f/h_p\right)T_f\right) + h_f T_f - JH_v}{h_m + h_f(1 + h_m/h_p)} \tag{21}$$

$$T_2 = \frac{h_m\left(T_f + \left(h_p/h_f\right)T_p\right) + h_p T_p + JH_v}{h_m + h_p(1 + h_m/h_f)} \tag{22}$$

where

$$h_m = \frac{k_m}{\delta_m} \tag{23}$$

5. Experiment and procedures

Experimental tests were performed using a PTFE membrane manufactured by Membrane Solution (85% porosity, 45 μm thickness, 0.22 μm nominal pore size). The main part of the used experimental set-up as shown in Fig. 3 is a plastic block (300 × 260 × 40) mm,

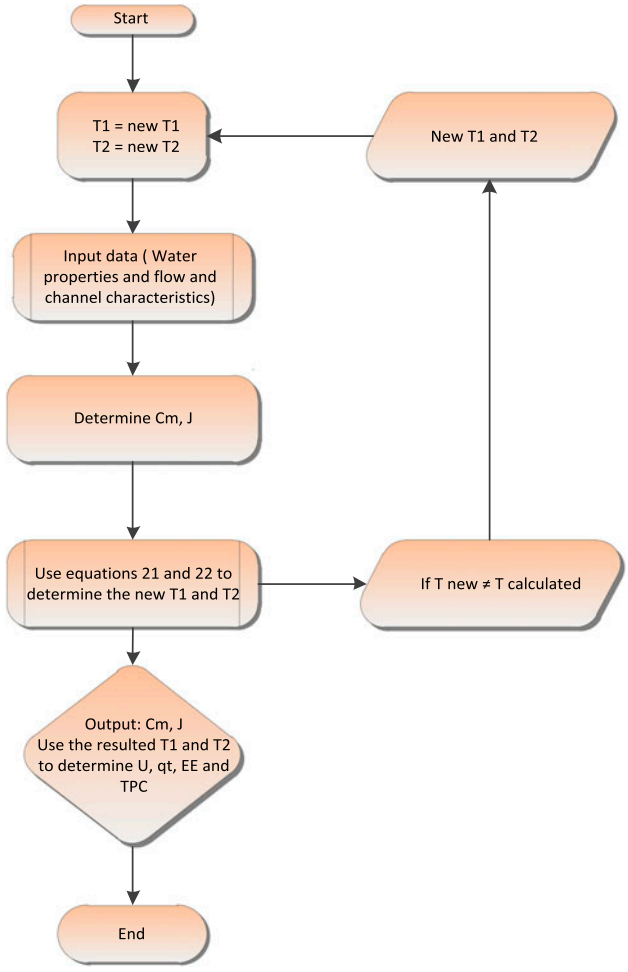

Fig. 2. The flow chart of the iterative computer method.

which is divided into two corresponded halves. The membrane sheet is placed between them, and a gap of 2 mm is provided between the membrane and the block surface to allow feed and permeate water flow. The effective membrane area for the transport was 0.0572 m, and it was supported by plastic net spacer. In all the experimental runs, the membrane was maintained in a horizontal position. The feed (saline water) was heated inside a container by thermostatic heater and then, pumped onto the membrane lower surface. The water at permeate side was cooled down by a water chiller in another container, then pumped onto the upper membrane surface. The recirculation flow at both sides of the membrane was in counter current directions. Temperatures of bulk liquid phases are measured at hot entrance (T_{f1}), cold entrance (T_{p1}), hot exit (T_{f2}) and cold exit (T_{p2}) of the membrane module. These temperatures will be different from the temperatures at the hot and cold membrane sides, T_1 and T_2, respectively. In this experimental set-up, permeate

Table 1
Sample of the mathematical model results

1% water salinity	ΔT = 40–20 = 20°C	ΔT = 50–20 = 30°C	ΔT = 60–20 = 40°C	ΔT = 70–20 = 50°C	ΔT = 80–20 = 60°C
Vmf (m/s)	0.075	0.075	0.075	0.075	0.075
Ref (DL)	451.6824635	537.037403	625.9795127	719.3270003	813.8408831
h_f (w/m^2 k)	907.1075953	918.7292894	927.339848	933.8611949	939.0185293
Vmp (m/s)	0.1136364	0.1136364	0.1136364	0.1136364	0.1136364
Rep (DL)	448.6522451	448.6522451	448.6522451	448.6522451	448.6522451
h_p (w/m^2 k)	1,006.336491	1,006.336491	1,006.336491	1,006.336491	1,006.336491
Path length (m)	0.0000033	0.0000025	0.0000019	0.0000015	0.0000012
Knudsen number (DL)	14.7966744	11.3900205	8.8493182	6.9382995	5.4852752
H_v (J/kg)	2,430,500	2,418,500	2,406,500	2,394,000	2,381,500
U (w/m^2 k)	329.551781	329.3346862	333.9580448	340.5471151	343.5595116
q_t (w/m^2)	6,591.03562	9,880.040586	13,358.32179	17,027.35576	20,613.5707
EE (DL)	0.1659413	0.1517676	0.1801499	0.2249557	0.2426144
TPC (DL)	0.3092237	0.3142714	0.30802	0.2969315	0.2927329
T_1 (k)	305.734009	312.2459719	318.5950094	324.7667167	331.0477487
T_2 (k)	299.5495346	302.81783	306.2742099	309.9201414	313.4837754
P_1 (P$_a$)	4,946.876824	7,083.141488	9,887.249055	13,476.52052	18,218.1184
P_2 (P$_a$)	3,458.530286	4,187.602948	5,099.868283	6,243.468444	7,568.386261
C_m (kg/m^2 P$_a$ s)	2.495E-07	2.475E-07	2.455E-07	2.436E-07	2.418E-07
J (kg/m^2 s)	0.00045	0.00062	0.001	0.0016	0.0021

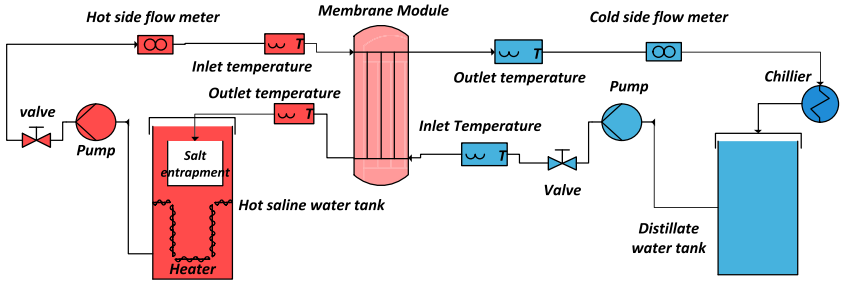

Fig. 3. MD experimental set-up.

water continuously collected in the distillate reservoir, and the corresponding distillate flux was measured by an electronic scale at the distillate reservoir. Furthermore, in this work, experiments were conducted with feed sodium chloride solutions of concentrations 0.1, 1, 3.7 and 20% of the density. Likewise, in all cases, the recirculation flow rates on both membrane surfaces were 2 L/m at feed side and 3 L/m at permeate side.

Different experiments were carried out for fixed temperatures in the membrane module. The feed temperature T_{f1} varied from 40 to 80°C at increments of about 10°C, and the cooling water temperature T_{p1} varied from 18 to 23°C.

6. Results and discussion

In Fig. 4, the distillate mass fluxes are presented as a function of temperature difference with different salt concentrations. These mass fluxes are the average value of at least three experiments obtained when temperatures $T_{f,in}$, $T_{f,out}$, $T_{p,in}$ and $T_{p,out}$ were recorded by connected thermocouples. The steady-state fluxes at different feed temperatures and salinities were also plotted against the vapour pressure differences ($\Delta P = P_1 - P_2$) calculated at the membrane surface temperatures (T_1, T_2) as shown in Fig. 5. The different pressure differences were determined at different salinities. The slope of the straight line is the MD coefficient, C = 0.001 kg/m^2 h P$_a$ (see Eq. (3)). C_m is a

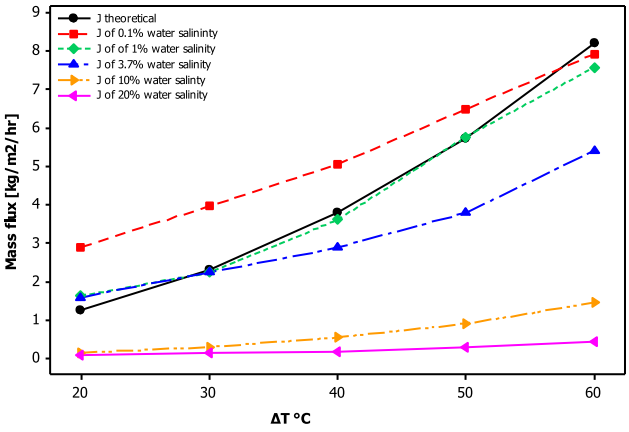

Fig. 4. Effect of temperature difference between feed and permeate side on membrane mass flux.

constant that relys on the membrane characteristics, and channel and vapour properties. The coefficient C_m may decrease due to the reduction of the surface area available for evaporation if the concentration polarisation and fouling exist. The value of C_m obtained in this study was less than that reported in the literature [6,14], which is due to low water flow at both sides of the membrane.

6.1. Effect of feed temperature

Fig. 6 compares the flux of distillate water and the feed side temperature. The increase of flux was depended on temperature at feed side, and the values were also in the reported range [15,18].

6.2. Effect of feed concentration

Mass flux decreased with increasing feed concentration (see Fig. 4). The decrease in vapour pressure is

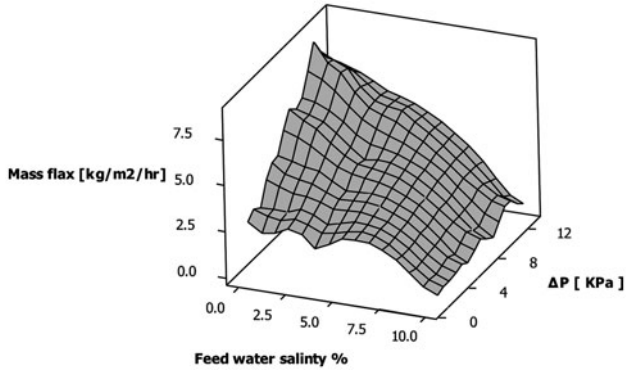

Fig. 5. Mass flux at different pressure differences and feed water salinities.

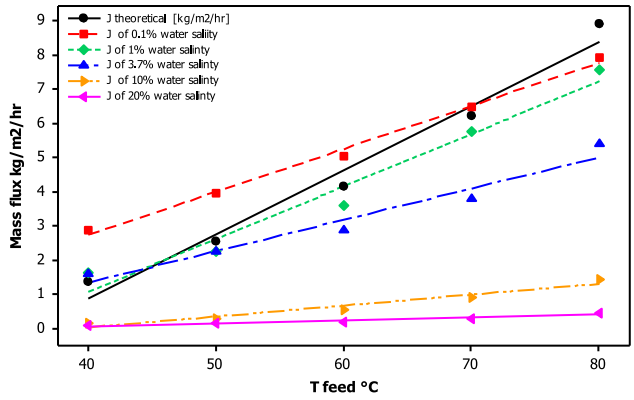

Fig. 6. Effect of feed side water temperature on permeation mass flux at different salinities.

the main cause and plays an important role. Flux decline over time was also observed, but it was more significant at high concentration. It suggested a possible effect of both concentration and temperature polarisation. The values of 0.27–0.3 TPC are shown in Fig. 7. The increase of retentate concentrations was examined and was found to be only 2–3% at 60˚C (after 9 h). Accordingly, concentration polarisation may be significant at high concentration, high temperature and at low flow rate. In this study, low flow rate was applied.

6.3. Evaporation correction factor

Due to the effect of water salinity concentration on its evaporation, the ratio between the evaporation rates of saline water to freshwater is empirically derived and used. The nomenclature for this ratio is K_{sc} (evaporation correction factor) such that;

$$K_{sc} = E_{\text{sal}}/E_{\text{fresh}} \tag{24}$$

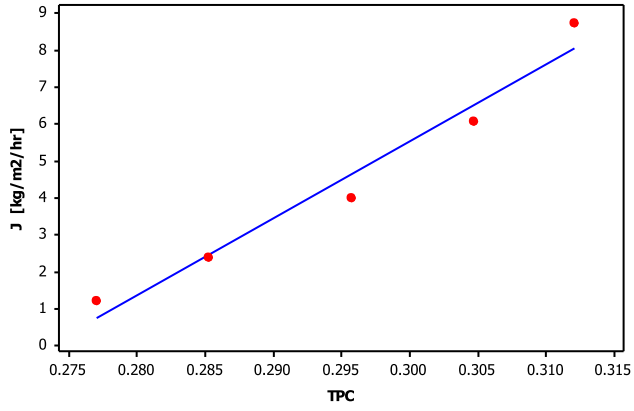

Fig. 7. The effect of TPC on membrane mass flux.

where K_{sc} ($0 < K_{sc} < 1$) is the reduction in evaporation due to salinity, E_{sal} is the rate of evaporation per unit area of saline water surface and E_{fresh} is the rate of evaporation per unit area of fresh water surface. Studies involving primarily inland saline water bodies have reported this ratio. Bonython and Warren [19] used thermally insulated evaporation pans over two summers to examine the effect of saline water with a density varying from 1.07 to 1.245 g/cm^3. He reported the ratio of salt water evaporation to freshwater evaporation as a function of the density of the solution. The resulted data are used in the comparison of the data reported later.

The assumption of exponential relation between salinity and evaporation rate can be used. Therefore, a correlation can be in the initial form of;

$$K_{sc} = ae^{\mathrm{Sab}} + c \tag{25}$$

where S is the water salinity, and a, b and c are the constants. Using values of S and K_{sc} that have been used practically by Pyramid Hill salt company in Australia, a, b and c can be determined. The resulted correlation is:

$$K_{sc} = 0.4e^{0.04S(\%)} + 0.6 \tag{26}$$

Fig. 8 shows the improvement in the predicted mass flux after incorporating the correlation in the computer model. It can be seen that new corrected J values have less deviation than the first theoretical values.

6.4. Analysis of heat transfer

The TPCs are presented in Fig. 7. The coefficients range from 0.27 to 0.32 for this study, indicating the higher effect of TPC on the heat balance. The low feed velocity resulted in lower TPCs. The reasons were given above. On the other hand, the TPC coefficients increased with feed temperature.

6.4.1. Heat transfer rates

The increase of heat energy transfer rate depends on the effect of h_f, which is less significant compared to the feed velocity effect. It is because of the dependency of latent heat (H_v) on feed water temperature [18]. At a constant feed temperature, the heat transfer at feed side was higher for more concentrated solutions, and it was related to lower permeation flux. In other words, with lower flux, the decrease of membrane surface temperature was not considerable. The heat transfer components are shown in Figs. 9 and 10. Heat fluxes increased with feed temperature, but decreased for higher concentration. This is in reasonable agreement with the above discussion. Considering that the heat transfer coefficient for the permeate stream is constant, it was observed that feed heat transfer in the membrane controlled the entire heat transfer system. Its rate is approximately 2–6 times higher than those of the vaporisation heat transfer rate. The percentage of conduction loss through the membrane was 71–85%; it increased with feed concentration, but decreased with increasing temperature.

6.4.2. Evaporation efficiency

Fig. 11 shows the effect of the temperature difference ΔT on the evaporation efficiency. Evaporation efficiency is defined as the ratio of the heat transferred by mass flux to the overall heat transferred in the

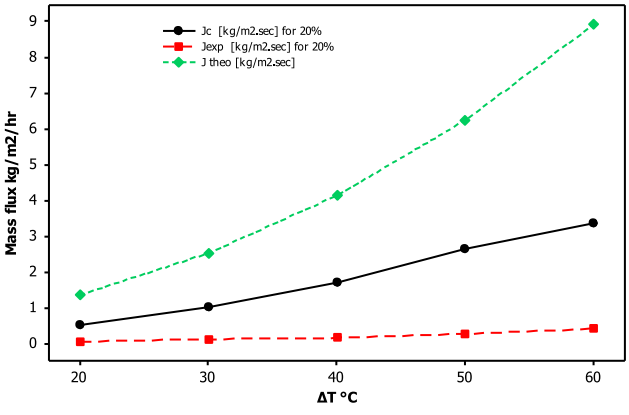

Fig. 8. Justified mass flux J after applying the correction factor on feed saline water with salinity of 20%.

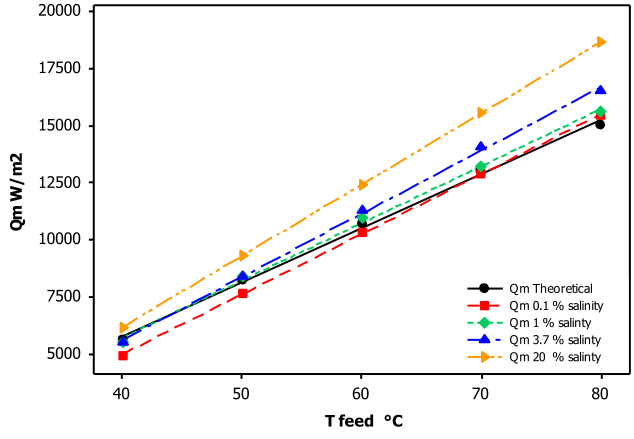

Fig. 9. Heat transfer rates through the membrane solid material.

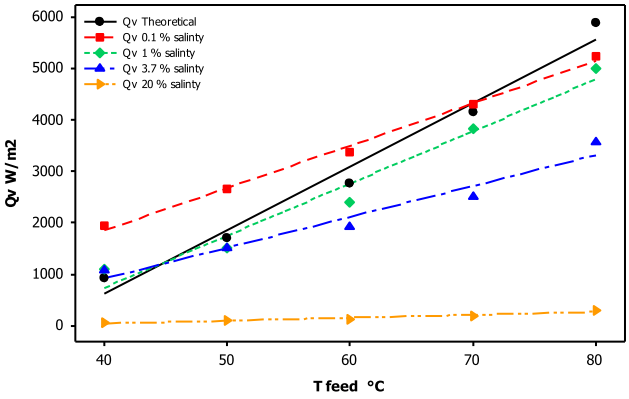

Fig. 10. Heat transfer rates by mass flux through the membrane.

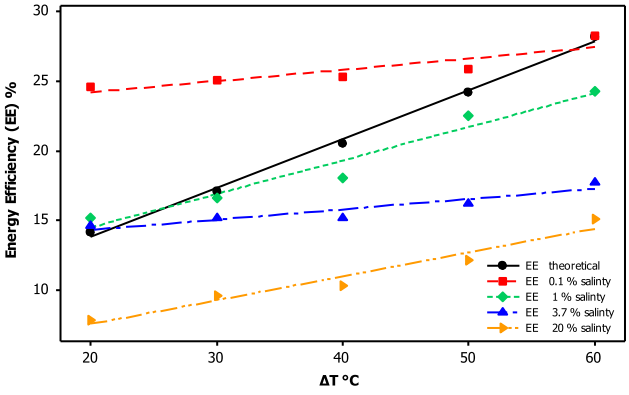

Fig. 11. Effect of temperature difference on evaporation efficiency with different concentrations.

membrane. As a result, the data shown in Fig. 10 represent, in addition to the evaporation efficiency, the mass transfer contribution to the overall heat transfer. This figure reveals that the evaporation efficiency as well as the mass transfer contribution to the overall heat transferred increase with the temperature difference increase. It is because the permeate water vapour flux exhibited an exponential increase with the temperature increase as discussed before. Overall, the EE values in Fig. 11 are low, and they are lower at lower operating temperatures. Therefore, the availability of sustainable energy such as solar energy might be the only solution to perform this process economically and make it feasible.

7. Conclusions

In this study, the heat transfer coefficients, the membrane heat transfer coefficients and the total heat transfer were calculated and predicted by the computer model. They were found to be at a good agreement with the experimental values. Also, an iterative solution was run and approximately determined the membrane/liquid interface temperatures, the membrane mass transfer coefficient and the evaporation efficiency using the experiments data. Measurements are also made at different operating temperatures with different feed concentrations.

The value of MD coefficient (C_m) obtained in this study was 0.001 $kg/m^2/s/P_a$, which is less than that reported in the literature. That is due to low water flow at both sides of the membrane. Also, the mass transfer contribution to the heat transfer was significant only in the membrane pores, while it was insignificant in both feed and permeates sides.

The permeate water flux, the evaporation efficiency, the membrane heat transfer coefficient and the transmembrane coefficient increase as the feed temperature is increased. Also, the mass transfer contribution to the overall heat transferred increases with the temperature difference increase. Whereas, the mass flux decreases with increasing of feed concentration as well as the evaporation efficiency.

In general, if working at lower temperatures is required, probably only the availability of cheap energy such as solar energy could make this process economically feasible. Finally, the prediction of the computer model was improved by using the evaporation correction factor especially for high water salinity concentrations.

Nomenclature

J	—	total mass flux of the membrane, $kg/m^2/h$
C_m	—	membrane mass flux coefficient, $kg/m^2\ P_a\ h$
C_{ap}	—	specific heat coefficient, J/kg K
P_1	—	vapour pressure at feed membrane surface, P_a
P_2	—	vapour pressure at permeate membrane surface, P_a
τ	—	membrane tortuosity
δ	—	membrane thickness, m
d	—	membrane pore diameter, m
ε	—	membrane porosity
R	—	gas constant, J/kg K
P_a	—	entrapped air pressure, P_a
M	—	molecular weight, kg/mol
T_f	—	bulk feed side temperature, K
T_P	—	bulk permeate side temperature, K
h_f	—	heat transfer coefficient at feed side, $W/m^2\ K$
h_p	—	heat transfer coefficient at permeate side, $W/m^2\ K$
h_m	—	heat transfer coefficient of the membrane, $W/m^2\ K$
Qv	—	latent heat transfer rate by vapour, W/m^2

References

[1] M.A. Hanjra, M.E. Qureshi, Global water crisis and future food security in an era of climate change, Food Policy 35 (2010) 365–377.

[2] P. Ranjan, S. Kazama, M. Sawamoto, A. Sana, Global scale evaluation of coastal fresh groundwater resources, Ocean Coastal Manage. 52 (2009) 197–206.

[3] M.R. Qtaishat, F. Banat, Desalination by solar powered membrane distillation systems, Desalination 308 (2013) 186–197.

[4] L. Mee, Between the Devil and the Deep Blue Sea: The coastal zone in an era of globalisation, Estuarine Coastal Shelf Sci. 96 (2012) 1–8.

[5] M. Khayet, Membranes and theoretical modeling of membrane distillation: A review, Adv. Colloid Interface Sci. 164 (2011) 56–88.

[6] H. Susanto, Towards practical implementations of membrane distillation, Chem. Eng. Process. 50 (2011) 139–150.

[7] M.S. El-Bourawi, Z. Ding, R. Ma, M. Khayet, A framework for better understanding membrane distillation separation process, J. Membr. Sci. 285 (2006) 4–29.

[8] C.M. Tun, A.M. Groth, Sustainable integrated membrane contactor process for water reclamation, sodium sulfate salt and energy recovery from industrial effluent, Desalination 283 (2011) 187–192.

[9] N. Ghaffour, T.M. Missimer, G.L. Amy, Technical review and evaluation of the economics of water desalination: Current and future challenges for better water supply sustainability, Desalination 309 (2013) 197–207.

[10] J.R.B. Rodríguez, V.M. Gabet, G.M. Monroy, A.B. Puerta, I.F. Barrio, Distilled and drinkable water quality produced by solar membrane distillation technology, Desalin. Water Treat. 51 (2012) 1265–1271.

[11] M. Khayet, C. Cojocaru, G. Zakrzewska-Trznadel, Studies on pervaporation separation of acetone, acetonitrile and ethanol from aqueous solutions, Sep. Purif. Technol. 63 (2008) 303–310.

[12] M. Khayet, Treatment of radioactive wastewater solutions by direct contact membrane distillation using surface modified membranes, Desalination 321 (2013) 60–66.

[13] M. Khayet, A. Velázquez, J.I. Mengual, Direct contact membrane distillation of humic acid solutions, J. Membr. Sci. 240 (2004) 123–128.

[14] D. Winter, J. Koschikowski, M. Wieghaus, Desalination using membrane distillation: Experimental studies on full scale spiral wound modules, J. Membr. Sci. 375 (2011) 104–112.

[15] A. Alkhudhiri, N. Darwish, N. Hilal, Membrane distillation: A comprehensive review, Desalination 287 (2012) 2–18.

[16] S. Srisurichan, R. Jiraratananon, A.G. Fane, Mass transfer mechanisms and transport resistances in direct contact membrane distillation process, J. Membr. Sci. 277 (2006) 186–194.

[17] F.P. Incropera, P.I. Frank, Fundamentals of Heat and Mass Transfer, Wiley, New York, NY, 2002.

[18] M. Qtaishat, T. Matsuura, B. Kruczek, M. Khayet, Heat and mass transfer analysis in direct contact membrane distillation, Desalination 219 (2008) 272–292.

[19] Bonython, C. Warren, Factors Determining the Rate of Solar Evaporation in the Production of Salt, in: Paper presented at the 2nd Northern Ohio Geological Society Symposium on Salt. Cleveland, Ohio, N. Ohio Geol. Soc. (1965) 152–165.